

Early Warning for the 2007 Noto Hanto Earthquake

Masumi YAMADA* and Jim MORI

* Pioneering Research Unit for Next Generation, Kyoto University

Synopsis

This paper applies different types of earthquake early warning algorithms to the dataset of the 2007 Noto Hanto Earthquake. Using the τ_c method (Wu and Kanamori, 2005) and the Virtual Seismologist method for large rupture dimension (Yamada, 2007), the magnitude of the earthquake and rupture geometry are estimated in an off-line simulation. The τ_c method provides an accurate estimate for the magnitude of the event, although the record for the closest station ISK006 gives an overestimate due to the long-period near-field term. The real time rupture geometry estimation agrees with the actual earthquake rupture geometry quite well. The rupture direction can be estimated 12 seconds after the event onset and the final solution is achieved after 15 seconds. These methodologies to characterize rupture geometry in real time were originally designed for larger earthquakes with larger rupture dimensions, but it is shown that they also work well for the size of the Noto Hanto earthquake (Mw 6.7).

Keywords: earthquake early warning, 2007 Noto Hanto Earthquake, fault finiteness, near-source ground motions.

1. Introduction

The 2007 Noto Hanto earthquake (Mw 6.7, Mj 6.9) produced strong shaking throughout central Japan with severe damage to over 600 buildings. The shallow event occurred close to the Japan Sea coast (37.22 N, 136.69 E, depth 10.7 km) on March 25, 2007 at 00:41:57.9 GMT. A significant number of near-source ground motions are recorded by the strong motion networks of Japan. The closest station to the epicenter is the K-NET station ISK006 (Togi), where the P- and S-wave arrived at 3 and 5 seconds after the origin time, respectively.

The early warning system of the Japan Meteorological Agency (JMA) issued a warning for the earthquake, but the warning arrived after the S-wave arrival in Wajima-city, Nanao-city, and Anamizu-town, which are the areas that were subjected to strong ground motions (Japan Meteorological Agency, 2007). For those cities, the

S-wave arrived 5 to 12 seconds after the origin time.

JMA reported the first warning was issued 9.9 seconds after the origin time from the single station estimate (Japan Meteorological Agency, 2007). The error of the warning was +0.1 for the magnitude, and 70 km for the epicentral location. A more reliable warning which used more than 2 records was issued 12.0 seconds after the origin time. The error in epicentral location for this information is much smaller, (<10 km), but magnitude was underestimated by 0.8. At that time, the S-wave had arrived at distances of 32 km from the epicenter.

This paper applies different types of earthquake early warning algorithms, in retrospect, to the dataset of the 2007 Noto Hanto Earthquake. Using the τ_c method (Wu and Kanamori, 2005) and the Virtual Seismologist method for large rupture dimensions (real-time inversion of acceleration envelopes and classification of near-source and

far-source records (Yamada, 2007)), the magnitude of the earthquake and rupture geometry are estimated in an off-line simulation. These methods could provide quicker warnings and rupture geometry information. Our final goal is to develop methods that will decrease the time for issuing warnings and increase the accuracy of the earthquake early warning.

2. Data

Strong motion data from the 2007 Noto Hanto earthquake were recorded by the K-NET and KiK-net strong-motion arrays, operated by the National Research Institute for Earth Science and Disaster Prevention (NIED) in Japan. More than 700 records are available at their websites (<http://www.k-net.bosai.go.jp/> and <http://www.kik.bosai.go.jp/>). Strong motion data were also recorded at the Japan Meteorological Agency (JMA) sites in the Noto area. Five significant records can be downloaded from the JMA website (<http://www.seisvol.kishou.go.jp/eq/>). From these datasets, 36 stations with epicentral distances less than 100 km are used for this analysis.

We use horizontal and vertical acceleration envelopes for the determination of rupture geometry. The horizontal components are calculated by the square root of sum of squares of the EW and NS components. Acceleration envelopes are obtained by taking the maximum absolute amplitude of the ground motion time history over a 1 second window.

3. Methods

τ_c method

For an earthquake early warning, it is important to estimate the size of an earthquake quickly. Wu and Kanamori (2005) developed a strategy to determine the magnitude of an earthquake from the first 3 seconds of strong motion records. Their τ_c method uses an average period during the first motion, which is computed by the following equation:

$$\tau_c = 2\pi \sqrt{\frac{\int_0^{\tau_0} u^2(t) dt}{\int_0^{\tau_0} \dot{u}^2(t) dt}}, \quad (1)$$

where $u(t)$ is vertical displacement high-pass filtered at 0.075Hz, and τ_0 is 3 seconds. Wu and Kanamori (2005) show an empirical relationship between the computed period and magnitude. The relationship between the moment magnitude (M_w) and average τ_c is given by;

$$\log \tau_c = 0.221M_w - 1.113. \quad (2)$$

For onshore events which occur in the upper crust, the JMA magnitude (M_j) and moment magnitude (M_w) have the following relationship (Takemura, 1990):

$$M_w = 0.78M_j - 1.08. \quad (3)$$

Substituting equation (3) into (2),

$$\log \tau_c = 0.172M_w - 1.352. \quad (4)$$

Real-time inversion for fault size

Information about the rupture dimension is useful to recognize areas subjected to severe ground shaking. We introduce a one-dimensional source model to express the fault finiteness based on the ground motion models constructed by Cua (2005). The length of the fault is divided into subsources, which are expressed as point sources (Fig. 1). The whole fault is parameterized by θ , N1, and N2, where θ is the azimuth of the strike of the fault and N1 (N2) is the number of subsources in the positive (negative) azimuthal direction.

Yamada (2007) constructed a ground motion model using acceleration envelopes for large earthquakes ($M_w > 6.5$). The ground motion at a station is expressed as a combination of the envelopes from each subsurface, and the ground motion model can be expressed as a function of the 3 fault parameters. The optimal parameters can be estimated by minimizing the error between the observed acceleration envelopes and predicted acceleration envelopes from the ground motion model. The error function, which is a measure of the goodness of fit, is defined as follows:

$$RSS(t) = \sum_{i=1}^{ns} \sum_{j=1}^2 \sum_{k=1}^t (A_{ijk} - \hat{A}_{ijk})^2, \quad (5)$$

where ns is the number of stations, t is the time in 1 second intervals ($\Delta t = 1$) from the event onset, A_{ijk} and \hat{A}_{ijk} are observed and predicted acceleration envelopes, respectively, of component (horizontal and vertical), at station i , at time $k\Delta t$. This nonlinear optimization problem is solved by the Neighborhood Algorithm (Sambridge, 1999a, b).

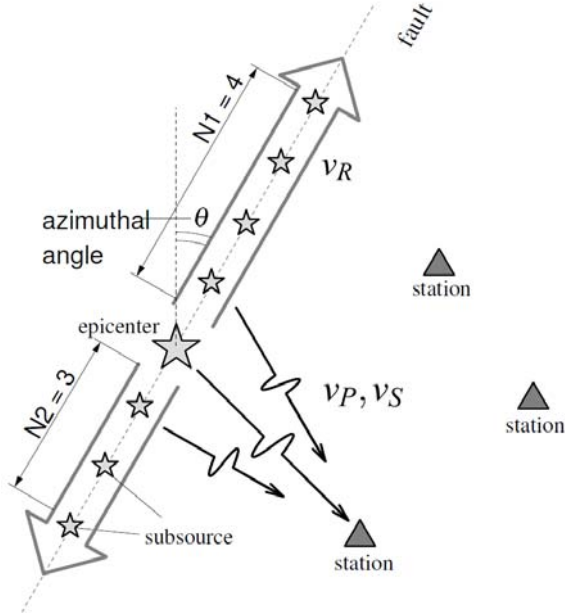


Fig. 1 Schematic diagram of the multiple source model. The fault rupture is assumed to propagate from the epicenter at a constant velocity. The fault is parameterized by θ , $N1$, and $N2$, where θ is the azimuth of the fault and $N1$ ($N2$) is the number of subsources in the positive (negative) azimuthal direction. The ground motion at a station is expressed as a combination of the envelopes from each subsurface.

Classification of near-source and far-source records

To estimate the fault dimensions of an earthquake in real time, Yamada et al. (2007) developed a methodology to classify seismic records into near-source or far-source distance ranges. A near-source station is defined to be a station with fault distance less than 10 km. Assuming the station distribution is sufficiently dense, the distribution of near-source stations is helpful for determining the rupture dimensions. The

discriminant function which shows the best performance is:

$$f_{disc} = 6.046 \log_{10} Za + 7.885 \log_{10} Hv - 27.091, \quad (6)$$

$$P(ns) = \frac{1}{1 + e^{-f_{disc}}}, \quad (7)$$

$$\text{If } \begin{cases} f_{disc} \geq 0 & ; \text{near-source,} \\ f_{disc} < 0 & ; \text{far-source,} \end{cases}$$

where Za and Hv denote the peak values of the vertical acceleration and horizontal velocity, respectively, and $P(ns)$ is the probability that a station is near-source. This function classifies near-source and far-source data, and gives the probability for a station to be near-field, based on the ground motion measurements.

4. Analysis and Results

Determination of magnitude

To determine the magnitude for earthquake early warning, the τ_c method is applied to the dataset of the Noto Hanto earthquake. The scaling law between τ_c and magnitude estimates for the mainshock and aftershock of the 2007 Noto Hanto Earthquake agree with the past observations of Wu and Kanamori (2005).

The first P arrival is recorded at the station ISK006 3.1 seconds after the origin time. Without considering data transfer latency, the first magnitude estimate can be obtained 6.1 seconds after the origin time. 10 sec after the origin time, the average estimate of the first 8 stations for the mainshock is M_j 7.1. Fig. 2 shows the magnitude estimate of each station for the mainshock. Most of the estimates are close to the final magnitude 6.9, and the standard deviation is 1.1. The closest station ISK006 is of particular interest, because it overestimates the magnitude significantly. This implies the predominant period of the first 3 seconds for the record is very long for this size of the earthquake. Fig. 3 shows the high-pass filtered displacement records of the closest 5 stations. The displacement record of ISK006 has a very long period component at the beginning. This is due to the near-field term, and this long period component can contaminate the magnitude estimate. The near-field term has not previously been considered

in source parameter determinations for earthquake early warning. However, these data suggest the importance in evaluating the effects of the near-field term.

Determination of rupture dimension

We have conducted the acceleration envelope inversion and near-source versus far-source classification technique to simulate an estimate of the rupture dimension in real time. We assume that

the location of the epicenter is already estimated from the other point-source method (Wu and Kanamori, 2005; Tsukada, 2004), and that the fault ruptures bilaterally from the epicenter with constant rupture velocity. The rupture velocity is assumed to be 3.0 km/s, and the magnitude of each subsource is Mw 6.2. These numbers are determined to minimize the error function in equation (5). The magnitude of the subsource roughly corresponds to the rupture area of the subsource.

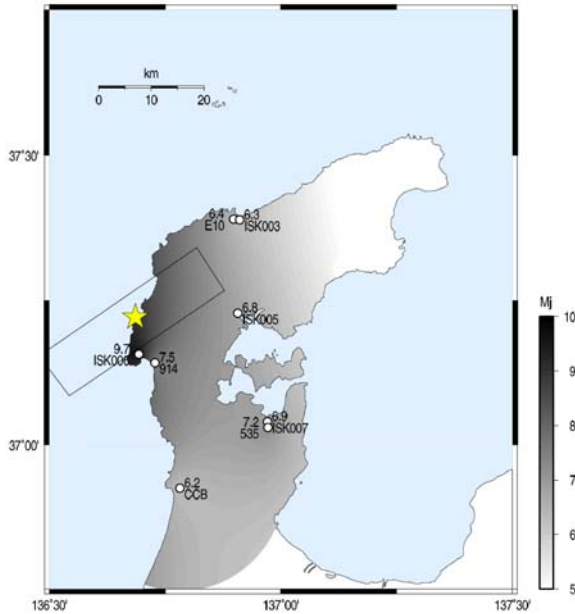


Fig. 2 Estimated single station magnitudes. The surface fault projection from Aoi and Sekiguchi (2007) is shown in solid lines. The star indicates the location of the epicenter.

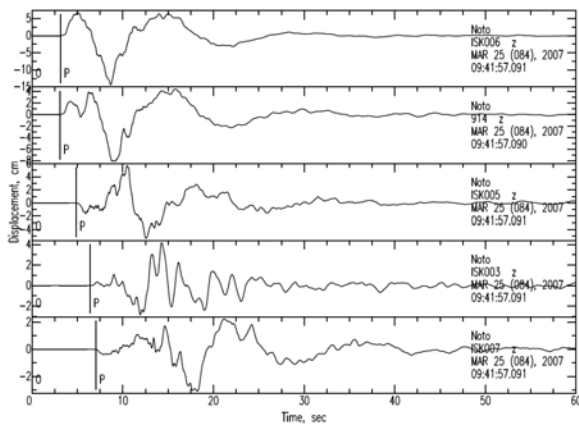


Fig. 3 Vertical component near-source displacements high-pass filtered at $0.075z$. The top panel is the record for the closest station ISK006, and clearly shows the near-field term.

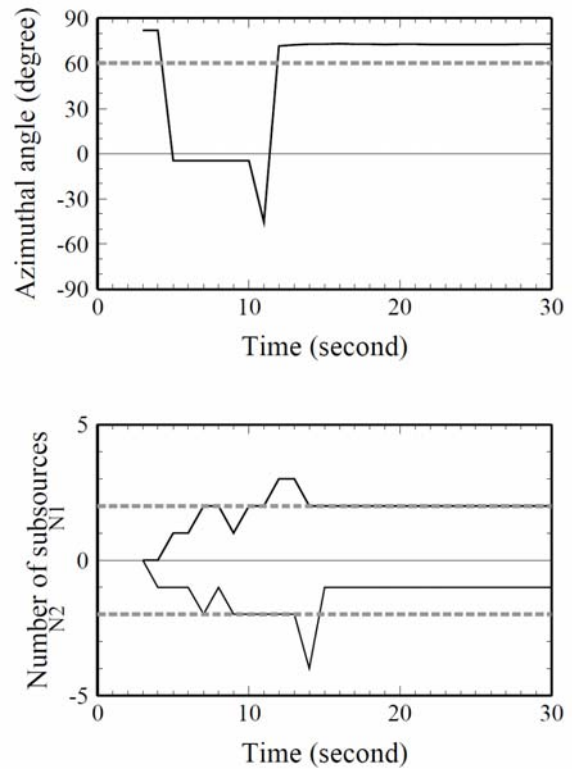


Fig. 4 Time series of the estimated parameters, θ , N_1 , and N_2 , for the source model. Time is relative to the earthquake origin time. The parameters are computed at one second intervals using only the data available at that time. The dotted lines are independent values based on the fault model proposed by Aoi and Sekiguchi (2007). Top: time series estimations for θ . Bottom: time series estimations for N_1 and N_2 .

Fig. 4 shows the estimation results of the three parameters (azimuthal angle of the fault line (θ), number of the point sources in the positive direction (N_1) and number of points in the negative direction (N_2)). The three parameters are computed

at one second intervals using only the data available at that time. The estimation is updated every second as the ground motion data are observed. The results show that the determination of the rupture direction (θ) converges to the final value at 12 seconds and is very close to a detailed fault model used for a waveform inversion (Aoi and Sekiguchi, 2007). On the other hand, the values of N1 and N2 increase as the rupture propagates, and finally stabilize after 15 seconds.

Fig. 5 shows a comparison of observed and predicted acceleration envelopes for the best fit source model. The model consists of 4 subsources distributed along a line trending 72 degrees clockwise from north; there are 2 subsources in the positive azimuthal direction and 1 subsurface in the negative azimuthal direction. The predicted acceleration envelopes for this model agree well with the observed envelopes. However, model envelopes at stations with soft soil condition (e.g. ISK005) underestimate the observations. Since the ground motions at soft soil sites are not explained by our simple ground motion model, it can contaminate the results of the inversion.

To classify records into near-source and far-source distances, the discriminant function in equations 6 and 7 is applied to 36 stations of the 2007 Noto Hanto earthquake strong motion dataset. We generated snapshots of the probability that a station is in the near-source region for times of 6, 10, and 15 seconds after the beginning of rupture. Peak ground motions used for this classification analysis are computed from the observed data every 5 seconds for each station and evaluated in the discriminant function. The results are shown in Fig. 6. A darker symbol at a station in Fig. 6 indicates that the station is more likely to be near-source, and a lighter mark indicates that the station is more likely to be far-source.

Six seconds after the rupture initiation, the map shows that stations with high probability of being in the near-source area are located near the epicenter. At 10 seconds, the number of darker symbols has increased, but it is still difficult to identify any directivity of the rupture propagation. At 15 seconds, the distribution of stations with high near-source probability agrees fairly well with the fault surface projection, and stations at the

near-source and far-source boundary have around 50% probability. The station distribution is not dense enough to characterize the size of the fault, but the classification results are in good agreement with fault model used for the waveform inversion.

5. Discussions and Conclusions

This paper applies different types of earthquake early warning algorithms to the dataset of the 2007 Noto Hanto Earthquake.

The τ_c method gives a magnitude estimate from the first 3 seconds of the waveforms. The magnitude estimate works very well for this earthquake, except for the closest station ISK006 due to the large amplitude near-field term. The effect of the near-field term does not show up for the magnitude estimate from JMA, since they use short-period amplitudes for the magnitude determination. Since the long-period character of the near-field term can contaminate the magnitude estimate in the τ_c method, it will be necessary to develop an algorithm which is not affected by the near-field term.

To reduce the time for issuing a warning, the computation time and data transfer latency are important. Most earthquake early warning systems can provide the magnitude and location estimates a few seconds after the origin time. The JMA early warning took only 3.6 seconds for the computation, but it took 6.3 seconds to catch the first p-wave arrival. Station density reduces the time to issue a warning, so increasing the number of real-time stations is the most direct way to quicken warning information.

For the Noto Hanto earthquake, the real-time inversion of acceleration envelopes was able to characterize the rupture geometry 15 seconds after the origin time. This is faster than the simulation for the 1999 Chi-Chi earthquake (Yamada, 2007), since the larger event has longer rupture duration and our method tracks the propagation of the rupture. For this simulation, we use a constant rupture velocity and constant magnitude of the subsources. However, we found these numbers affect the fault parameter estimates. Therefore, we need to include these parameters into the inversion parameters for future work.

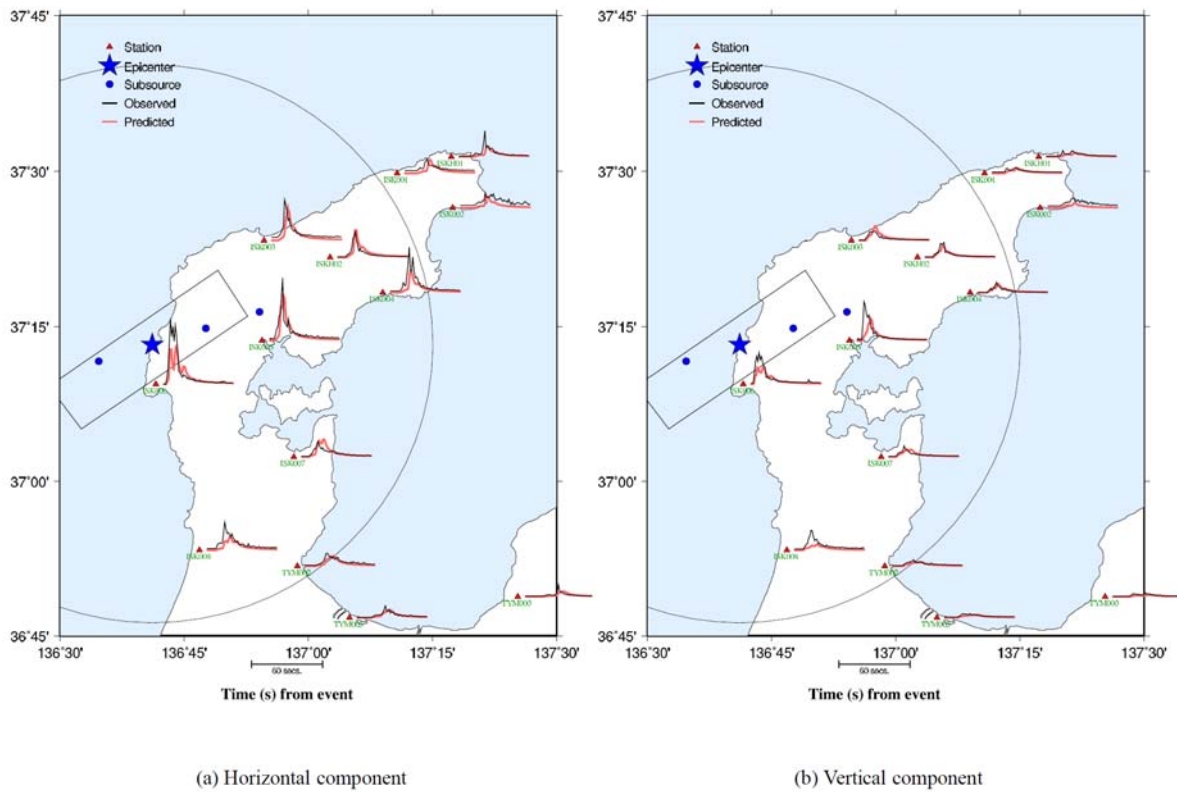


Fig. 5 Predicted and observed acceleration envelopes for the horizontal components. The gray and black lines are the predicted and observed envelopes, respectively. The locations of the subsources estimated from the simulation are shown in small circles. The area within 50 km from the epicenter is shown by large circles. The surface fault projection from Aoi and Sekiguchi (2007) is shown by the box. Only characteristic records of the stations are shown in this figure.

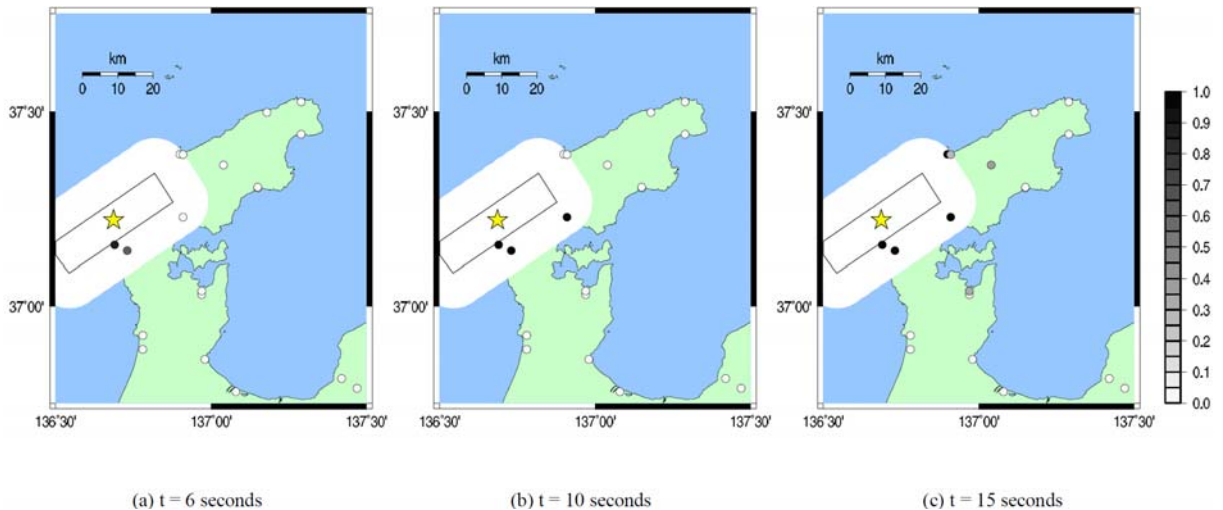


Fig. 6 Snapshots of the probabilities of near-source for the 2007 Noto Hanto earthquake. Darker symbols for a station indicate that the station is more likely to be near-source. The surface fault projection from Aoi and Sekiguchi (2007) is shown by the box. The white area around the fault projection indicates the area with distance less than 10 km from the fault projection, which is the area of near-source.

The time-dependent classification of data into near-source versus far-source distances also tracks the rupture propagation, and the near-source region extends as the rupture propagates. The classification performance for the Noto Hanto Earthquake was very high, and only one station near the boundary between the near-source and far-source regions was mis-classified.

These methodologies to characterize rupture geometry in real time were originally designed for large earthquakes with larger rupture dimension, but it is shown that they can work for earthquakes the size of the Noto Hanto event (Mw 6.7). For small earthquakes, it may not be necessary to determine the rupture dimension, since the source can be generally characterized as a point source. However, these results show that the rupture geometry characterized by these methods agrees well with the fault model from waveform inversions.

Acknowledgements

The authors thank Tomotaka Iwata and Kimiyuki Asano of Kyoto University for supporting the damage survey. We thank Hiroo Kanamori of California Institute Technology and Yih-Min Wu of National Taiwan University for helpful discussions and technical guidance. We acknowledge NIED and JMA for the use of the strong motion data. This research was supported by the Program for Improvement of Research Environment for Young Researchers from Special Coordination Funds for Promoting Science and Technology (SCF) commissioned by the Ministry of Education, Culture, Sports, Science and Technology (MEXT) of Japan.

References

Aoi, M. and H. Sekiguchi (2007): Source inversion from the near-source ground motions for the 2007 Noto Hanto Earthquake, <http://www.kyoshin.bosai.go.jp/k-net/topics/noto070325/2007> (in Japanese).

Cua, G. (2005): Creating the Virtual Seismologist : Developments in ground motion characterization and seismic early warning, Ph.D. thesis, California Institute of Technology.

Japan Meteorological Agency (2007): The report of the early warning for the 2007 Noto Hanto Earthquake, <http://www.seisvol.kishou.go.jp/eq/EEW/kaisetsu/200608/joho.html>, (in Japanese).

Sambridge, M. (1999): Geophysical inversion with a neighbourhood algorithm - I. Searching a parameter space, *Geophys. J. Int.*, 138, 479–494.

Sambridge, M. (1999): Geophysical inversion with a neighbourhood algorithm - II. Appraising the ensemble, *Geophys. J. Int.*, 138, 727–746.

Takemura, M. (1990): Magnitude-seismic moment relations for the shallow earthquakes in and around Japan, *Zisin2*, 43, 257–265, (in Japanese with English abstract).

Tsukada, S., S. Odaka, K. Ashiya, K. Ohtake and D. Nozaka (2004): Analysis of the Envelope Waveform of the Initial Part of P Waves and its Application to Quickly Estimating the Epicentral Distance and Magnitude, *Jisin2*, 56, 351–361, (in Japanese).

Wu, Y. M. and H. Kanamori (2005): Experiment on an Onsite Early Warning Method for the Taiwan Early Warning System, *Bull. Seism. Soc. Am.*, 95, 257–265.

Yamada, M. (2007): Early Warning for Earthquakes with Large Rupture Dimension, Ph.D. thesis, California Institute of Technology.

Yamada, M., T. Heaton, and J. Beck (2007): Real-Time Estimation of Fault Rupture Extent Using Near-Source versus Far-Source Classification. *Bulletin of the Seismological Society of America*, No.97-6, pp.1890-1910.

2007年能登半島地震における緊急地震速報

山田 真澄*・Jim MORI

*京都大学次世代開拓研究ユニット

要 旨

本稿は、2007年能登半島地震の強震記録に、異なる緊急地震速報アルゴリズムを適用したものである。 τ_c 法 (Wu and Kanamori, 2005) と、大断層のためのVirtual Seismologist 法 (Yamada, 2007) を用いて、能登半島地震のマグニチュードや断層領域をオフラインシミュレーションで推定した。その結果、 τ_c 法によって推定されたマグニチュードは正確であったが、最も震源に近い観測点ISK006では、長周期の近地項のためにマグニチュードは過大評価となった。リアルタイムでの断層領域の推定は、波形インバージョンで使用された実際の断層面とよい一致を示した。破壊方向は破壊開始時刻から12秒後に推定でき、15秒後に最終的な解に収束した。これらのリアルタイムで断層領域を推定する手法は、本来より断層面の大きい大地震に対して構築されたものであるが、能登半島地震のサイズの地震(Mw 6.7)でもよく推定できることが示された。

キーワード: 緊急地震速報, 2007能登半島地震, 断層の有限性, 強震動